

Grating coupled liquid crystal waveguides using nematics and smectics

G. P. Bryan-Brown, J. R. Sambles, and K. R. Welford

Citation: *Journal of Applied Physics* **73**, 3603 (1993); doi: 10.1063/1.352918

View online: <http://dx.doi.org/10.1063/1.352918>

View Table of Contents: <http://scitation.aip.org/content/aip/journal/jap/73/8?ver=pdfcov>

Published by the [AIP Publishing](#)

Articles you may be interested in

[Induced smectic phases in phase diagrams of binary nematic liquid crystal mixtures](#)

J. Chem. Phys. **134**, 124508 (2011); 10.1063/1.3567100

[Prism grating using polymer stabilized nematic liquid crystal](#)

Appl. Phys. Lett. **82**, 3168 (2003); 10.1063/1.1573366

[The reorientational behavior of nematic and smectic liquid crystals in a magnetic field](#)

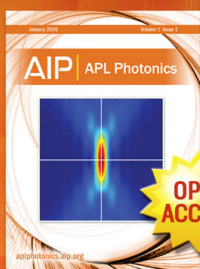
J. Chem. Phys. **100**, 1470 (1994); 10.1063/1.466626

[Flexoelectricity in nematic and smectic-A liquid crystals](#)

J. Appl. Phys. **47**, 2298 (1976); 10.1063/1.323021

[Optical waveguide modulation using nematic liquid crystal](#)

Appl. Phys. Lett. **22**, 365 (1973); 10.1063/1.1654675



Launching in 2016!

The future of applied photonics research is here

OPEN
ACCESS

AIP | APL
Photonics

Grating coupled liquid crystal waveguides using nematics and smectics

G. P. Bryan-Brown^{a)} and J. R. Sambles

Thin Film and Interface Group, Department of Physics, University of Exeter, Exeter, Devon EX4 4QL, United Kingdom

K. R. Welford

Defence Research Agency, Malvern, Worcestershire WR14 2PS, United Kingdom

(Received 2 November 1992; accepted for publication 22 December 1992)

The optical properties of grating coupled waveguides are theoretically modeled and practically demonstrated using nematic and smectic liquid crystals as thin ($0.7\ \mu\text{m}$) waveguide layers. Voltage induced reorientation of the liquid crystal is shown to lead to large changes in reflectivity and transmissivity when the angle of incidence initially corresponds to a guided mode resonance. Time resolved measurements using these thin cells show that the switching time for the nematic phase can be faster than the smectic phase.

INTRODUCTION

Corrugated multilayer structures have many uses one of which is the ability to couple light into resonant guided modes which can exist in a layer if it is bounded by layers of lower refractive index and has a thickness greater than $\lambda/4n$ (Ref. 1) (where λ is the wavelength and n is the waveguide refractive index). Such structures may act as narrow band optical filters² separating light of different wavelengths or of different angles of incidence. However, to make a tunable filter or a modulator, the waveguide layer must have voltage-addressable optical properties. Aligned liquid crystals are an obvious choice for such a layer as they exhibit large changes in optical properties which can be driven with low voltages.

Liquid crystal waveguide structures have previously been constructed using prism couplers^{3,4} through such devices are rather bulky, and thus, inconvenient for many applications. In this work, we extend a previous investigation⁵ and study a grating coupled waveguide structure incorporating a layer of either a nematic (BL016) or a smectic (mix 783) liquid crystal. The grating serves the double purpose of coupling light into waveguide modes while also homogeneously aligning the liquid crystal. The cell is simple, rugged, and can be cleaned and refilled many times. Optical properties of these cells are examined by recording reflectivity and transmissivity versus incident angle and switching speeds are measured by time resolved experiments.

THEORY

The corrugated waveguide may be modeled as a high refractive index layer (liquid crystal) sandwiched between two low refractive index diffraction gratings of sinusoidal profile as shown in Fig. 1. There should be a large difference between the waveguide refractive index (n_2) and the cladding refractive index (n_1) to ensure large diffraction efficiency. The lowest index cladding material that can be easily used in practice is MgF_2 ($n=1.38$). In modeling, we assume an infinite cladding layer but in practice the MgF_2

layers need only be thick enough to extend beyond the evanescent fields of the guided modes. The uniaxial liquid crystal is modeled as an isotropic layer which is valid in the case of the homogeneously aligned nematic and smectic A phases when the optic axis lies perpendicular to the plane of incidence.

For this configuration it is of particular interest to calculate the zeroth order reflected and transmitted signals since it is these that are measured experimentally. Such calculations are carried out using rigorous differential grating theory.⁶ This corrugated system does not possess unique directions for surface tangents and normals, hence, it is difficult to apply the simple electromagnetic boundary conditions. Therefore, in the differential formulation a nonorthogonal coordinate transformation is carried out which maps the grating surface into a planar system. Incoming and scattered beams along with Maxwell's equations are then reexpressed in this coordinate frame in which the system may be solved.

Figure 2 shows the theoretically generated reflectivity and transmissivity for TE polarized light ($\lambda=632.8\ \text{nm}$) from a system with a grating pitch of 800 nm and a groove depth of 50 nm. The cladding layers have an optical permittivity, ϵ of 1.9044 ($=n_1^2$) while the liquid crystal layer has $\epsilon=2.890+0.0001i$ and a thickness of $1\ \mu\text{m}$ (it is assumed that the liquid crystal lies with its director parallel to the grating grooves). The excitation of a guided mode (in this case the TE_2 mode) is clearly shown by a peak in the normally low reflectivity and a dip in the normally high transmissivity. Excitation of such modes occurs at angles of incidence, θ , such that

$$nk \sin \theta + k_g = k_{\text{GM}}, \quad (1)$$

where n is the index of the bounding media (glass), k_g is the reciprocal grating vector, $k=2\pi/\lambda$, and k_{GM} is the guided mode propagation wave vector.

A voltage induced reorientation of the liquid crystal can be approximately modeled as a drop in layer permittivity (for example $\epsilon=2.873+0.0001i$) which causes the mode excitation to move to lower angles as shown in Fig. 2 by dashed lines. (This is only a valid approximation for small reorientations as large changes must be modeled us-

^{a)}Present address: DRA, Malvern, Worcs, UK.

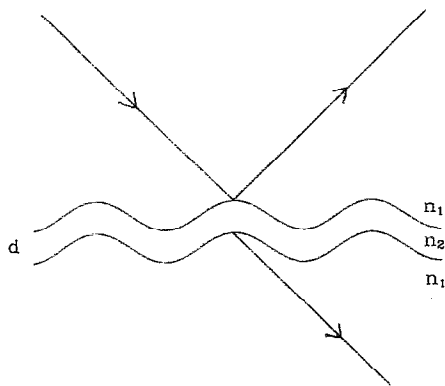


FIG. 1. Waveguide structure consisting of a higher index layer sandwiched between two lower index parallel aligned gratings.

ing a tilted uniaxial model which in the grating formulation is currently not possible.) If the angle is fixed at 31.63° , then the application of a voltage will cause a rise in transmissivity (from 0.002 to 0.991) and a drop in reflectivity (from 0.916 to 0.001). In practice this could be used as a high contrast modulator, which may be utilized in reflection or transmission. In addition to this, the grating coupler is highly wavelength dispersive and so in Fig. 2 the range of angles may be replaced by wavelength. Hence, the configuration could also be used to split off an adjustable wavelength band (with a FWHH of 0.65 nm) from a polychromatic input beam. The grating groove depth used for the curves in Fig. 2 has been optimized in order to give an on-resonance transmission close to zero. Figure 3 shows plots of the minimum transmissivity (dotted lines) and the maximum reflectivity (solid lines) as a function of groove depth for three different values of the waveguide ϵ_i . For case A ($\epsilon_i=0.0001$) the dip in transmission is close to zero for a wide range of groove depths; hence good contrast may be obtained. An ϵ_i of 0.001 (case B) also allows good extinction of the transmitted beam but shows a reduction in the peak reflectivity. A highly absorbing waveguide with $\epsilon_i=0.005$ (case C) shows poor extinction for any groove depth. Hence, these curves show that liquid

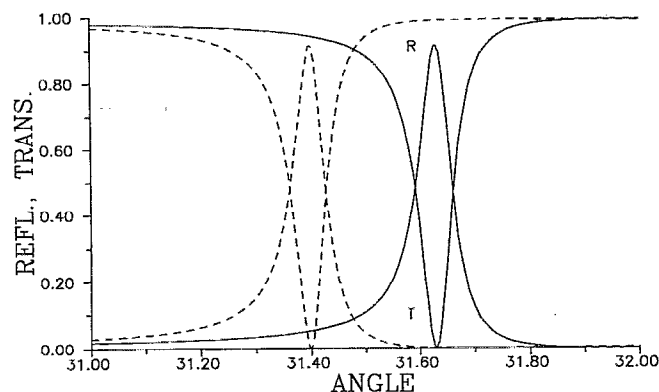


FIG. 2. Theoretical transmissivity and reflectivity of TE polarized light as a function of angle for a waveguide permittivity of 2.890 (solid lines) and 2.873 (dashed lines).

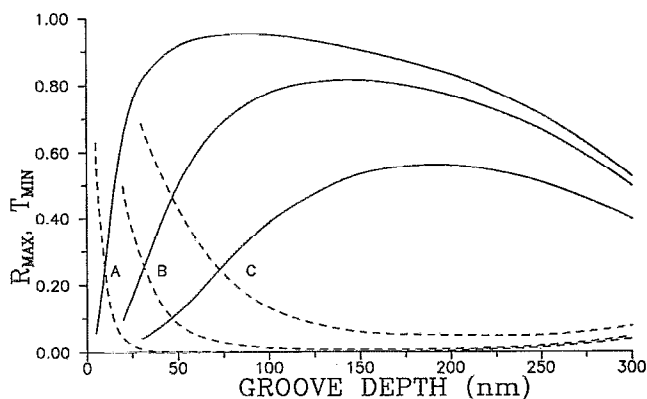


FIG. 3. Maximum reflectivity (solid lines) and minimum transmissivity (dashed lines) at the guided mode resonance as a function of groove depth for three different values of the waveguide ϵ_i . (A) 0.0001; (B) 0.001; (C) 0.005.

crystal waveguide layers must have a total absorption (scattering and intrinsic) corresponding to an ϵ_i of no more than 0.001 in order to be used as high contrast modulators or wavelength selectors.

EXPERIMENT

The grating substrate and superstrate which enclose the liquid crystal are made by a standard interferographic technique.⁷ Indium tin oxide (ITO) coated float glass with a resistance of $240 \Omega/\square$ is cleaned and spin-coated with AZ 1350 photoresist (diluted 1:1 in thinners) at a rate of 2000 rpm. The photoresist is dried in an oven and then exposed to interfering beams from an argon ion laser operating at 457.9 nm. Once exposed the sample is developed in microposit developer for 10 s leaving a sinusoidal grating profile in the resist. Gratings used here typically have a groove depth to pitch ratio of between 0.1 and 0.2.

A 100 nm layer of MgF_2 is next vacuum evaporated onto the photoresist in order to protect the photoresist from being dissolved by the liquid crystal and also to act as a low index waveguide cladding layer. The waveguide is then constructed by placing the gratings face to face with the grating grooves parallel and capillary filling in a clean environment with the liquid crystal at an appropriate temperature. A high degree of parallelism ($<0.01^\circ$) of the grating grooves (and hence, alignment direction) is obtained by making small adjustments to one of the gratings while viewing the moiré-interference fringe pattern in the overlapping diffracted beams. (This is particularly important for smectic alignment.) Once filled the cell is clamped tightly without mylar spacers to give a thickness of $\sim 0.7 \mu\text{m}$.

The waveguides are studied by recording the zeroth order (specular) reflectivity and transmissivity of polarized light from a HeNe laser ($\lambda=632.8 \text{ nm}$) as a function of incident angle under appropriate electrical bias. Time resolved data are also taken in order to deduce switching speeds.

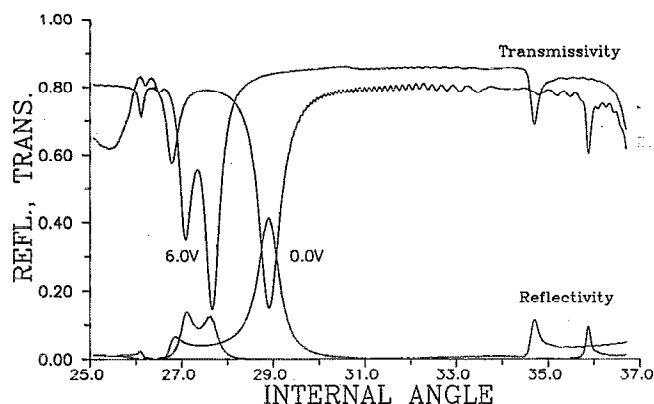


FIG. 4. Experimental reflectivity and transmissivity of TE polarized light as a function of angle from a cell filled with nematic BL016.

Once all data had been taken the cell was dismantled, cleaned, and the gratings were coated with an opaque layer of silver to allow grating characterization by the excitation of surface plasmon polaritons.⁸

RESULTS

The first cell to be constructed was filled with Licrilit BL016 nematic liquid crystal (obtained from Merck, Poole, UK). This liquid crystal has a nematic phase at room temperature which extends up to 83°. The cell was filled at room temperature and examination between crossed polarizers showed uniform homogeneous alignment across the entire grating surface (1.5 cm × 1.5 cm). The gratings were later characterized and were both found to have a peak to trough groove depth of 109.0 ± 0.4 nm and a pitch of 743.2 ± 0.5 nm.

Figure 4 shows the reflectivity and transmissivity of TE polarized light from the cell as a function of angle. The azimuthal angle is set so that the grating grooves are perpendicular to the plane of incidence. With no applied bias a TE₀ mode is excited at 35.9°, the TE₁ is excited at 29.0°, and the TE₂ mode is excited at 26.8° (the angle range refers to the internal inside the bounding glass layers). Further scans are also shown in Fig. 4 which were taken with an applied ac bias of 6.0 V rms. The ac frequency was chosen to be 5 kHz to avoid beating effects with the 1.7 kHz modulation that is applied to the optical beam for phase sensitive detection purposes. Under an electrical bias the liquid crystal which is originally aligned with its major optic axis parallel to the grating grooves undergoes a Fredericksz deformation tilting out of the plane of the substrate. Hence, the effective index seen by TE polarized modes decreases, and they move to lower angles as seen in Fig. 4. The TE₁ mode appears to be split by the applied voltage, however the lower angle resonance (at 27.1°) is in fact a TM-like mode which is coupled to the TE mode in this tilted uniaxial system. When the cell is switched the reflectivity at 28.9° falls from 0.413 to 4.5 × 10⁻⁴. A large change in transmission is also seen but with a much smaller contrast.

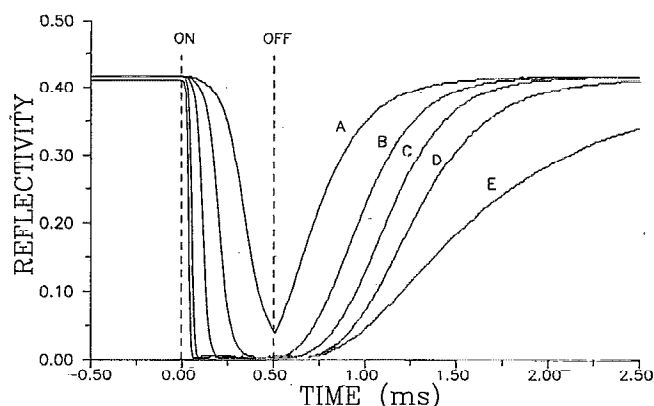


FIG. 5. Time-resolved data showing the reflectivity response of the BL016 cell during the application of dc pulses of various peak voltages. (A) 3.50 V; (B) 4.50 V; (C) 6.09 V; (D) 10.00 V; (E) 13.28 V.

The switching speed of the cell was measured by fixing the angle of incidence at 28.9° and measuring the reflectivity during the application of 0.5 ms dc pulses separated by 16.5 ms. Figure 5 shows the time resolved response for pulses of various voltages. Switch-on and switch-off times (10%–90%) are measured from these scans and plotted against voltage as shown in Fig. 6. Switch-off times (circles) increase linearly with pulse voltage which is due solely to charging effects in the cell. The switch-on time for a Fredericksz deformation for small deviations from the initial orientation is given by⁹

$$\frac{1}{\tau_{on}} = \frac{\pi^2 K_{11}}{d^2 \gamma_1 (1 - \alpha_s)} \left[\left(\frac{V}{V_0} \right)^2 - 1 \right], \quad (2)$$

where V is the applied voltage, V_0 is the threshold voltage, d is the cell thickness, γ_1 is the rotational viscosity and $(1 - \alpha_s)$ is a correction for backflow effects which is close to 1 for a splay deformation. The curve in Fig. 6 is a fit to data (stars) using the above equation with V_0 set to 0.71 V and $[\pi^2 K_{11}/d^2 \gamma_1 (1 - \alpha_s)]$ set to 182 s⁻¹. Using known values for γ_1 (0.57 Pa s, Merck data sheet) and d (1.0 μm) and assuming that $(1 - \alpha_s) \approx 1$, we get a value of 10.5 × 10⁻¹² N for K_{11} . To our knowledge this is the first time

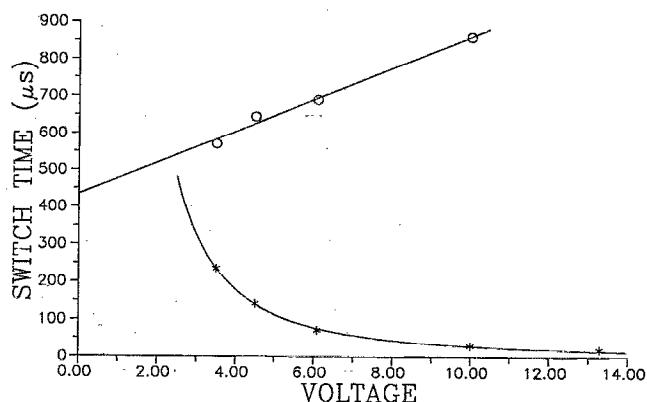


FIG. 6. Switch-on (stars) and switch-off (circles) time as a function of the applied dc voltage. The theoretical fit to the former is obtained using Eq. (2).

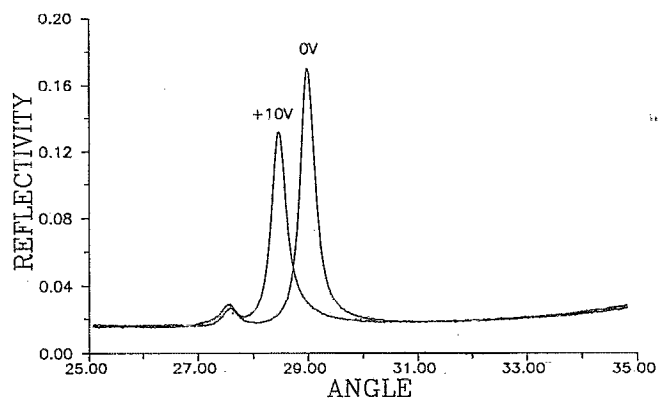


FIG. 7. Experimental reflectivity of TE polarized light as a function of angle from a cell filled with smectic C* mix 783.

that K_{11} has been measured for BL016. However, a similar material, BL015 has a K_{11} value of 14.6×10^{-12} N and so our result obtained for BL016 is probably a little low.

A similar liquid crystal cell was constructed with mix 783 (from Merck) which has a smectic C* phase at room temperature. Filling of the cell was carried out in the nematic phase (92° – 116°) followed by slow cooling to room temperature. A smectic A phase from 92° to 61.2° helped alignment during cooling to result in a well aligned smectic C* phase in which the major optic axis was twisted off from the grating grooves by a constant angle across the entire grating region. Therefore, it is expected that incident TE polarized light will respond to a combination of ϵ_{\parallel} (2.81) and ϵ_{\perp} (2.23). Figure 7 shows reflectivity scans from the cell using TE polarized light. The scan with no applied field shows a TE_0 guided mode at 29° and a TE_1 guided mode at 27.5° . The lower angles of these modes compared to the BL016 cell shows that they are indeed detecting a lower refractive index. If a dc bias of +10 V is now applied then its interaction with the spontaneous polarization will cause an increase in twist and also a nonzero tilt. This reduces the refractive index detected by the modes and so moves them to lower angles as shown in Fig. 7. (The TE_1 mode is less sensitive to changes in waveguide index which is normal for a mode with a propagation index close to the refractive index of the bounding media.) A similar effect is seen with an applied bias of -10 V.

The switching speed of the cell was measured by setting the angle of incidence to the peak of the TE_0 mode (0 V) and then recording the reflectivity and transmissivity during the application of 1.0 ms, +10 V pulses separated by 23.2 ms. The pulse shifts the waveguide to an off-resonance state and so causes a drop in reflectivity and a rise in transmissivity as shown in Fig. 8. Switch-on and switch-off times are 32 and 175 μ s, respectively. An alternative temporal response can be obtained by applying a square wave bias centered ~ 0 V. In this case, the waveguide is only on-resonance, when the voltage sweeps through 0 V and so a set of sharp temporal spikes are obtained as shown in Fig. 9. The applied square wave had a period of 2.0 ms and a peak to peak voltage of 23.28 V. Downward going and upward going voltages (at $t=1.0$ ms

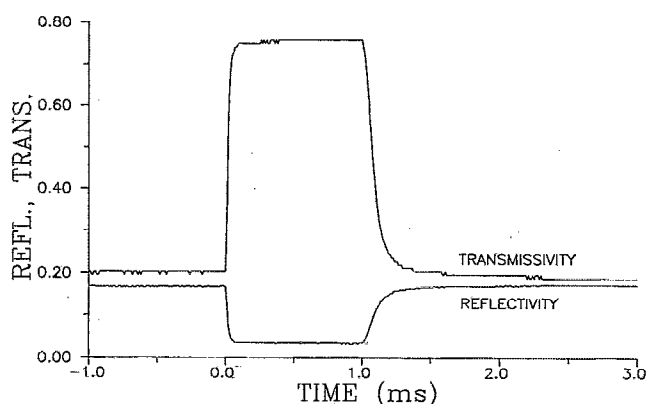


FIG. 8. Time-resolved data showing the reflectivity and transmissivity response of the mix 783 cell during the application of a 13.28 V dc pulse on a background of 0 V.

and $t=2.0$ ms) produce slightly different times. Taking the average lead to a rise time of 28 μ s and a fall time of 30 μ s.

DISCUSSION

In this work a grating coupled waveguide has been modeled in which the incident beam excites a guided mode which in turn reradiates into the reflected beam leading to an enhancement of the reflectivity and a reduction in transmissivity. As with all grating coupled systems, it is the groove depth that dictates the coupling strength; however, efficient coupling is ultimately limited by waveguide absorption (either intrinsic or scattering).

A practical waveguide configuration has been demonstrated which is both simple and rugged. (Cells may be cleaned and refilled many times without loss of alignment quality.) A 0.7 μ m thick nematic cell showed uniform alignment and was found to have a thickness spread of less than ± 0.1 μ m. The throughput of the device is reduced to $\sim 85\%$ (off-resonance) due to absorption in the ITO and the photoresist layers, but this could be improved by etching the grating profile into a silica substrate and coating with higher quality ITO. However, this cell did show high contrast in reflection ($\sim 920:1$). Time resolved experi-

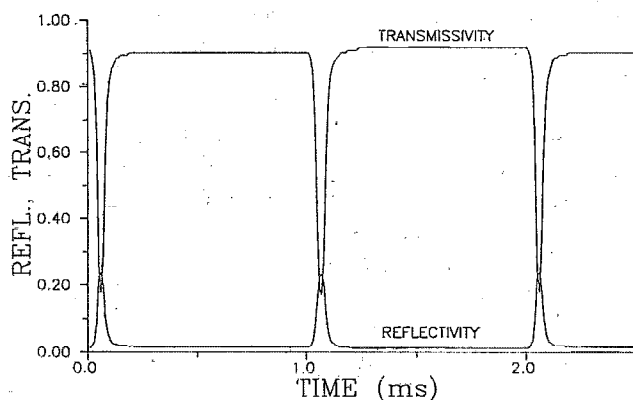


FIG. 9. Time-resolved data showing the reflectivity and transmissivity response of the mix 783 cell during the application of a ± 23.28 V square wave.

ments showed that thin nematic cells can take full advantage of the d^2 switch time dependence displaying switch-on times as fast as 20 μs . (This compares closely with an 18 μs switch time obtained from an E7 waveguide in a previous experiment.⁵) The switch-off time can be improved by using ac rather than dc pulses, thus, avoiding charging effects, but even then the relaxation would still take 435 μs (see Fig. 6). However, if a two frequency nematic is used the cell can be driven into the off state with switch times closer to $\sim 20 \mu\text{s}$.

A smectic C^* cell has also shown good alignment with the accuracy of parallelism between the gratings ensuring that the smectic layers are continuous across the sample. The smectic C^* phase is more ordered than the nematic phase and so less scattering (hence, absorption) is expected. This is indeed shown by narrower guided modes. The decreased efficiency in reflection is due to the lower refractive index sensed by the guided modes which is further decreased in the +10 V scan when further twist occurs. Time resolved scans showed a switching time of 30 μs when driven and a relaxation time of 175 μs . Other studies of smectic C^* waveguides have shown a switch time of 200 μs for a 2 μm cell³ and 4 μs for a 4 μm cell.⁴ Therefore, unlike nematics there is no clear advantage in building very thin cells except that thinner cells can be switched by lower voltages. However, accurate comparison between different results is difficult as optical switch times can be much faster than the liquid crystal reorientation time.

In conclusion, the use of shallow diffraction gratings

has been shown to be a reliable method for aligning both nematic and smectic liquid crystals and also coupling light into waveguide modes. Electric field induced reorientation perturbs the modes and leads to large changes in reflectivity and transmissivity even though the samples are thin ($\sim 0.7 \mu\text{m}$). Further improvements should lead to lower waveguide absorption, and hence, perfect extinction of the transmitted beam as shown theoretically in Fig. 2. By using thin cells, it has also been shown that nematics can be made to switch faster than smectics; however, the long switch-off time of the former must still be improved.

ACKNOWLEDGMENTS

G. B.-B. acknowledges DRA (Malvern) for their support of a postdoctoral fellowship.

¹S. L. Chuang and J. A. Kong, *J. Opt. Soc. Am.* **73**, 669 (1983).

²G. M. Gallatin, *Proc. SPIE* **815**, 158 (1987).

³N. A. Clark and M. A. Handschy, *Appl. Phys. Lett.* **57**, 1852 (1990).

⁴M. Ozaki, Y. Sadohara, T. Hatai, and K. Yoshino, *Jpn. J. Appl. Phys.* **29**, L843 (1990).

⁵G. P. Bryan-Brown, J. R. Sambles, and K. R. Welford, *Liq. Cryst.* (to be published).

⁶J. Chandezon, M. T. Dupuis, G. Cornet, and D. Maystre, *J. Opt. Soc. Am.* **72**, 839 (1982).

⁷M. C. Hutley, *Diffraction Gratings* (Academic, London, 1982), pp. 95-124.

⁸G. P. Bryan-Brown, S. J. Elston, and J. R. Sambles, *J. Mod. Opt.* **38**, 1181 (1991).

⁹M. Schiekkel, K. Fahrenschon, and H. Gruler, *Appl. Phys.* **7**, 99 (1975).